

Magnetic Properties and New Structural Classification of Molybdenum Phosphates Containing Mo(V)

E. Canadell,[†] J. Provost,^{*,‡} A. Guesdon,[‡] M. M. Borel,[‡] and A. Leclaire[‡]

Laboratoire CRISMAT-CNRS URA 1318, ISMRA/Université de Caen,
Boulevard du Maréchal Juin, 14050 Caen Cedex, France, and Institut de Ciencia de Materials
de Barcelona (CSIC), Campus de la UAB, 08193 Bellaterra, Spain, and Laboratoire de
Structure et Dynamique des Systèmes Moléculaires et Solides, Université de Montpellier II,
34095 Montpellier Cedex, France

Received February 28, 1996. Revised Manuscript Received July 15, 1996[®]

A combined theoretical and experimental study of molybdenum phosphates containing Mo(V) either as purely Mo(V) or as mixed-valent Mo(V)/Mo(VI) and Mo(IV)/Mo(V) is performed. This investigation, based on a structural classification of molybdenum phosphates, derived from that proposed by Costentin et al., allows a detailed discussion of both the valence of the different Mo sites as well as the different coupling mechanisms for the unpaired electron of the Mo(V) octahedra. Either direct Mo–Mo or indirect interaction through the shared oxygen atoms can lead to magnetic moments per Mo(V) lower than expected. It is shown that although the PO₄ tetrahedra do not effectively couple the unpaired electrons of the different Mo(V)O₆ octahedra, they play an important role in determining the magnetic properties of these solids by influencing the internal geometry of the MoO₆ octahedra.

Introduction

Recent work on the molybdenum phosphates has shown a great ability of the phosphate matrix to stabilize pentavalent molybdenum. Despite the original features of the host lattices, they are all structurally interrelated and are characterized by a specific geometry of the MoO₆ octahedra, typical of the molybdenyl cation.

In 1992, Costentin et al.¹ proposed a classification based on the number of octahedra sharing their corners or their edges in the “Mo–P–O” frameworks. They distinguished class I, involving only isolated octahedra, from class II in which there exist infinite chains of corner-sharing MoO₆ octahedra, with class III corresponding to the compounds built up of polyoctahedral Mo units. Since 1992, new Mo(V) phosphates have been discovered that exhibit structural units built up of several octahedra. Moreover, some of these units exhibit molybdenum with different valences. This is the case of the A₂Mo₂O₃(PO₄)₂ monophosphates with A = K, Rb, Tl,^{2–4} A₃Mo₄O₆(PO₄)₄ with A = Tl, Rb,⁵ and Cs_{1.5}Mo₂O₃(PO₄)₂⁶ that are all characterized by Mo₂O₁₁ units built up of two corner-sharing MoO₆ octahedra; in these phosphates molybdenum is pentavalent for the first series, whereas a mixed valence Mo(V)–Mo(VI) is observed for the second series. Similarly, the phosphate

AMo₃O₆(PO₄)₂⁷ is of great interest since one of its octahedral sites may contain either Mo(V) or Mo(VI) depending on the valence of the A cation inserted between the layers. In this case the different valences seem to be located on specific molybdenum sites, but as will be shown below, this is not always the case.

To progress in our understanding of the crystal and electronic structure of these phases, we propose a structural classification, based on that proposed by Costentin et al.¹ but which is more general. The latter is then used for the experimental and theoretical study of the magnetic properties of these phases in order to discuss in detail the valence of the different molybdenum sites in these solids.

Experimental Section

Synthesis. The syntheses of the different compounds were performed in two steps, starting from a mixture in stoichiometric ratios to obtain the considered formula. First, a mixture of H(NH₄)₂PO₄, MoO₃, a nitrate or a carbonate of the particular monovalent or divalent cation, and Al(NO₃)₃·9H₂O in the case of the molybdenum aluminophosphates was ground and heated to 673 K in air in order to decompose the nitrate or carbonate and the ammonium phosphate. In the second step, the resulting finely ground powder was mixed with the appropriate amount of molybdenum. This sample was sealed in an evacuated silica ampule, heated for 12 h to a temperature ranging from 793 to 1173 K (Table 1) and finally quenched to room temperature. The X-ray diffraction spectra of all the powdered compounds studied hereafter were systematically registered and did not show any impurity phase. To check the absence of an amorphous phase, all the samples were carefully examined using a optical binocular microscope (×40). No amorphous phase could be detected in any sample.

Magnetic Measurement. The magnetic moments of the samples were measured by SQUID magnetometry. The signal was registered with a 4 cm length scan under a field of 1 T. After zero field cooling a magnetic field was applied at *T* =

[†] Institut de Ciencia de Materials de Barcelona and Laboratoire de Structure et Dynamique des Systèmes Moléculaires et Solides.

[‡] Université de Caen.

[®] Abstract published in *Advance ACS Abstracts*, November 1, 1996.

(1) Costentin, G.; Leclaire, A.; Borel, M. M.; Grandin, A.; Raveau, B. *Rev. Inorg. Chem.* **1993**, *13*, 77.

(2) Gueho, C.; Borel, M. M.; Grandin, A.; Leclaire, A.; Raveau, B. *J. Solid State Chem.* **1993**, *104*, 202.

(3) Guesdon, A.; Leclaire, A.; Borel, M. M.; Grandin, A.; Raveau, B. *Acta Crystallogr.*, in press.

(4) Guesdon, A.; Borel, M. M.; Grandin, A.; Leclaire, A.; Raveau, B. *Acta Crystallogr.* **1993**, *C49*, 1877.

(5) Borel, M. M.; Leclaire, A.; Guesdon, A.; Grandin, A.; Raveau, B. *J. Solid State Chem.* **1994**, *112*, 15.

(6) Borel, M. M.; Leclaire, A.; Grandin, A.; Raveau, B. *J. Solid State Chem.* **1994**, *108*, 336.

(7) Borel, M. M.; Guesdon, A.; Leclaire, A.; Grandin, A.; Raveau, B. *Z. Anorg. Allg. Chem.* **1994**, *620*, 569.

Table 1. Synthesis of the Studied Samples

compound	synthesis temp (K)	result
CsMoO(P ₂ O ₇)	873	Cs(MoO)(P ₂ O ₇) ^a and β-CsMo ₂ P ₃ O ₁₃ as impurity
KMoO(P ₂ O ₇)	1100	green powder
α-A ₂ Mo ₂ O ₃ (PO ₄) ₂ (A = K, Rb)	973	red powder
Rb ₃ Mo ₄ O ₆ (PO ₄) ₄	933	khaki powder
CdMoO ₂ (PO ₄)	1173	purple powder
β-K ₂ Mo ₂ O ₄ (P ₂ O ₇)	923	brown powder
AgMo ₃ O ₆ (PO ₄) ₂	873	dark blue powder
SrMo ₃ O ₆ (PO ₄) ₂	993	brown powder
A ₉ Mo ₉ O ₃ (AlO ₄) ₃ (PO ₄) ₁₁ (A = Cs, Rb, K/Cs, Rb/Cs)	973	brown powder
CsMo ₂ O ₂ (PO ₄) ₂	1093	brown powder
Cs ₆ Mo ₇ O ₉ (PO ₄) ₇ ·H ₂ O	793	brown powder

^a The magnetic measurements were performed on a sample consisting of green crystals of CsMoO(P₂O₇) picked out with tweezers using a binocular microscope.

4.5 K, and the measurements were performed up to 350K. The magnetic signal of the sample holder was measured in the same conditions. This signal and the core magnetic contributions of the different ions of the structure were subtracted. The resultant component of the magnetic moment parallel to the applied field, M_z , can be written

$$M_z = (m/M)\chi_M H$$

where m is the sample mass, M is the molar mass of the compound, χ_M is the molar susceptibility, and H is the magnetic field.

Structural Classification

Taking into consideration the great complexity of the frameworks of the phosphates involving molybdenum(V), we have chosen a very easy system of classification based only on the number of MoO₆ octahedra, i.e., each group of the classification includes the phosphates in which the frameworks exhibit the same number of octahedra in their octahedral unit. Thus group 1 includes all the compounds exhibiting the isolated octahedra, group 2 the compounds having a biotetrahedral unit, group 3 the phosphates showing a triotetrahedral unit, etc. and finally group ∞ contains the compounds with [MoO₅]_∞ infinite octahedral chains. Each group is split into subgroups according to the type of sharing in the octahedral unit (corner sharing or edge sharing). If a compound has two sorts of octahedral units in its framework, the latter is enclosed in the group corresponding to the unit built from the greater number of octahedra. Table 2 summarizes this classification.


This new system of classification of the molybdenum(V) phosphates is more flexible than that previously published. Indeed, it is possible to easily include structures exhibiting new octahedral units. Moreover, the establishment of relations between the physical properties and the structure of these compounds required a comparison between the different frameworks and particularly between the different types of units involved in these frameworks. The comparison is easier with this classification as shown by the magnetic study in which the possible coupling between molybdenum atoms is very important.

Magnetic Study


The results of the magnetic measurements (Table 3) are presented here following the new classification of

Table 2. Structural Classification

* Group 1 : Isolated octahedron MoO₆

1a : only MoO₆ 

α-KMo₂P₃O₁₃⁸
 γ-KMo₂P₃O₁₃⁹
 α-CsMo₂P₃O₁₃¹⁰
 BaMo₂P₄O₁₆¹¹
 β-AMo₂P₃O₁₃ (A = K¹², Rb¹³, Tl¹⁴, Cs¹⁰)
 γ-CsMo₂P₃O₁₃¹⁵
 e-NaMo₂P₃O₁₃¹⁶
 ξ-AMo₂P₃O₁₃ (A = Na¹⁷, Ag¹⁸)
 Mo₂P₄O₁₅¹⁹
 AMoO(P₂O₇) (A = K²⁰, Cs²¹, Li²²)
 CsMo₂O₃(PO₄)₂²³


1b : MoO₆ linked to one bipyramid MoO₅ (Mo₂O₁₀ unit) 

AMo₃O₄(PO₄)₃ (A = Na, Ag, Li)²⁴⁻²⁶

* Group 2 : biotetrahedral unit


2A : two MoO₆ octahedra linked by one corner : Mo₂O₁₁ unit 

α-A₂Mo₂O₃(PO₄)₂ (A = K², Rb³, Tl⁴ and cationic mixture K/Cs, K/Rb, Rb/Cs²⁷)
 Cs_{1.5}Mo₂O₃(PO₄)₂⁶
 A₃Mo₄O₆(PO₄)₄ (A = Rb, Tl)⁵
 Li_xMo₂O₃(PO₄)₂ (x = 0.2)²⁸
 LiMo₂O₃(PO₄)₂²⁹

2B : two MoO₆ octahedra linked by one edge : Mo₂O₁₀ unit 


2B₁ : isolated Mo₂O₁₀ unit

β-K₂Mo₂O₄(P₂O₇)³⁰
 Na₃Mo₂P₂O₁₁(OH)₂H₂O³¹
 AMoO₂(PO₄) (A = Cd³², Fe³³)

2B₂ : Mo₂O₁₀ unit linked to one bipyramid MoO₅ (Mo₃O₁₄ unit) 


AMo₃O₆(PO₄)₂ (A = K, Ag, Na, Rb and Sr)⁷

* Group 3 : triotetrahedral unit

3A : one MoO₆ octahedron shares an apex with one Mo₂O₁₀ unit : Mo₃O₁₅ unit 

A₉Mo₉O₃(AlO₄)₃(PO₄)₁₁ (A = Cs³⁴, Rb, and cationic mixtures K/Cs et Rb/Cs³⁵)

* Group 4 : tetraoctahedral unit

4A : one MoO₆ octahedron shares an apex with one Mo₃O₁₅ unit : Mo₄O₂₀ unit 

4A₁ : isolated Mo₄O₂₀ unit

A_{2-y}Mo₂O₂(PO₄)₂·xH₂O (y = 0.5 with A = K, Rb, Tl³⁶ and y = 1 with A = NH₄³⁷, Rb³⁸, Cs³⁶)
 Cs₆Mo₇O₉(PO₄)₇·H₂O³⁹

4A₂ : Mo₄O₂₀ unit linked to one tetrahedron MoO₄

Cs_{8+x}(MoO₄)Mo₁₂O₁₈(PO₄)₁₀·H₂O⁴⁰

4B : Mo₄O₁₆ unit 

BaMo₄O₈(PO₄)₂⁴¹

* Group ∞ : infinite chain of MoO₆ octahedra linked by corner sharing

(chain of type [MoO₅]_∞)

AgMo₅P₃O₃₃⁴²
 MoPO₅⁴³
 MoAlP₂O₉⁴⁴

Table 2. These results will be discussed in more detail in the next section where, on the basis of the results of a molecular orbital study, we try to correlate the structural and magnetic properties of these phases. It is interesting to remind here that some of the polyhedral units are obtained with mixed valent molybdenum.

Isolated Octahedral Units. Isolated octahedra Mo(V)O₆ are present in the structures of the compounds CsMoOP₂O₇²¹ and KMoOP₂O₇.²⁰ The Mo(V)O₆ octahe-

(8) Leclaire, A.; Monier, J. C.; Raveau, B. *J. Solid State Chem.* **1983**, *48*, 147.

(9) Leclaire, A.; Borel, M. M.; Grandin, A.; Raveau, B. *Z. Kristallogr.* **1989**, *188*, 77.

(10) Lii, K. H.; Haushalter, R. C. *J. Solid State Chem.* **1987**, *69*, 320.

(11) Costentin, G.; Borel, M. M.; Grandin, A.; Leclaire, A.; Raveau, B. *J. Solid State Chem.* **1990**, *89*, 83.

(12) Leclaire, A.; Borel, M. M.; Grandin, A.; Raveau, B. *Acta Crystallogr.* **1990**, *C46*, 2009.

Table 3. Magnetic Measurements Results^a

compound	χ_0 (emu mol ⁻¹)	θ (K)	C_M	$\mu_{\text{eff}} = \mu/\mu_B$ per Mo(V) ion
CsMoO(P ₂ O ₇) ($T > 25$ K)	-0.0003	-43.5	0.211	1.30
KMoO(P ₂ O ₇) ($T > 25$ K)	0	-27	0.375	1.73
α -K ₂ Mo ₂ O ₃ (PO ₄) ₂	0.000086	-4	0.025	0.22
Rb ₂ Mo ₂ O ₃ (PO ₄) ₂	0.000118	4.5	0.005	0.10
Rb ₃ Mo ₄ O ₆ (PO ₄) ₄	0.00080	-0.2	0.296	0.51
CdMoO ₂ (PO ₄)	0.000045	-8.5	0.0038	0.17
β -K ₂ Mo ₂ O ₄ (P ₂ O ₇)	0.00012	-10	0.057	0.34
AgMo ₃ O ₆ (PO ₄) ₂ ($T > 25$ K)	-0.00022	-12.	0.275	1.48
SrMo ₃ O ₆ (PO ₄) ₂	0.000155	-11	0.023	0.22
Cs ₉ Mo ₉ O ₃ (AlO ₄) ₃ (PO ₄) ₁₁	0.002	-6	0.717	0.27
K ₂ Cs ₇ Mo ₉ O ₃ (AlO ₄) ₃ (PO ₄) ₁₁	0.037	-25	1.146	0.34
Cs ₄ Rb ₅ Mo ₉ O ₃ (AlO ₄) ₃ (PO ₄) ₁₁	0	-16.4	1.093	0.33
Rb ₉ Mo ₉ O ₃ (AlO ₄) ₃ (PO ₄) ₁₁	0.008	-17	1.047	0.32
CsMo ₂ O ₂ (PO ₄) ₂	0	-5.5	0.357	0.85
Cs ₆ Mo ₇ O ₉ (PO ₄) ₇ ·H ₂ O	0.0005	4.7	0.588	0.43

^a Temperature: 4.5 K $\leq T \leq$ 300 K, Magnetic field: 1 T.

dra are strongly distorted: one of the distances between the molybdenum and the apical oxygen atoms is short (less than 1.7 Å), whereas the other is very long (about 2.2 Å).

The molar susceptibility of these two compounds versus the temperature T are plotted in Figure 1. The curve corresponding to the potassium compound shows an antiferromagnetic ordering at $T \approx 25$ K. The two curves have been fitted with a Curie–Weiss type law:

$$\chi_M = \chi_0 + \frac{C_M}{T - \theta}$$

The fitting parameter C_M leads to 1.30 μ_B per Mo atom for CsMoOP₂O₇ and 1.73 μ_B for KMoOP₂O₇. These values should be compared to 1.73 μ_B , the theoretical value computed for a spin-only contribution and $g = 2$. The experimental value found for the Cs-based molybdenum phosphate is significantly lower than the theoretical one. As the structures of the K- and Cs-based compounds are very similar, it is difficult to find a decisive reason to explain this difference.

Biocahedral Units. Following the classification introduced in the present paper, we have found three different behaviors of the magnetization for these molybdenum phosphates. These differences can be ascribed to the difference in the biocahedral units (classes 2A, 2B₁, 2B₂) and to the mixed valence or not of the molybdenum atoms in these units.

(a) *Class 2A:* In this class the biocahedral units Mo₂O₁₁ are built up from two corner-sharing octahedra.

In α -K₂Mo₂O₃(PO₄)₂² and α -Rb₂Mo₂O₃(PO₄)₂³ the two molybdenum atoms have the same valency, Mo(V). From the slopes of the $(\chi_M - \chi_0)^{-1}$ versus T curves we

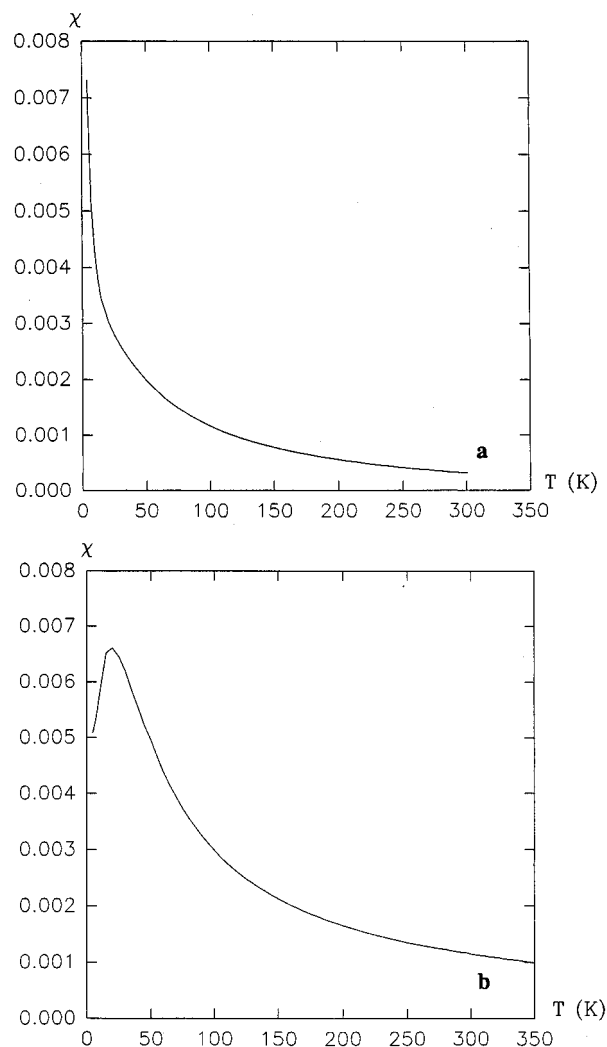


Figure 1. Molar susceptibility χ versus temperature T of two class 1a compounds: (a) CsMoO(P₂O₇) shows a paramagnetic behavior in the whole range of temperature investigated here (4.5–300 K) with 1.30 μ_B per Mo(V). (b) KMoO(P₂O₇) showing an antiferromagnetic ordering at $T \approx 25$ K. Fitting the paramagnetic domain with a Curie–Weiss law leads to 1.73 μ_B per Mo(V).

find 0.22 and 0.10 μ_B per Mo(V) for the K- and Rb-based compound respectively (Figure 2). This nearly diamagnetic behavior is discussed in the following section.

In the Rb₃Mo₄O₆(PO₄)₄ compound, we have two crystallographically independent Mo₂O₁₁ biocahedral units,

- (13) Riou, D.; Goreaud, M. *J. Solid State Chem.* **1989**, *79*, 99.
 (14) Costentin, G.; Borel, M. M.; Grandin, A.; Leclaire, A.; Raveau, B. *Acta Crystallogr.* **1991**, *C47*, 1136.
 (15) Chen, J. J.; Lii, K. H.; Wang, S. L. *J. Solid State Chem.* **1988**, *76*, 204.
 (16) Leclaire, A.; Borel, M. M.; Grandin, A.; Raveau, B. *J. Solid State Chem.* **1990**, *89*, 10.
 (17) Costentin, G.; Borel, M. M.; Grandin, A.; Leclaire, A.; Raveau, B. *J. Solid State Chem.* **1990**, *89*, 31.
 (18) Hoareau, T.; Borel, M. M.; Grandin, A.; Leclaire, A.; Raveau, B. *C. R. Acad. Sci.* **1994**, *319*, 47.
 (19) Costentin, G.; Borel, M. M.; Grandin, A.; Leclaire, A.; Raveau, B. *Z. Kristallog.* **1992**, *201*, 53.
 (20) Gueho, C.; Borel, M. M.; Grandin, A.; Leclaire, A.; Raveau, B. *Z. Anorg. Allg. Chem.* **1992**, *615*, 104.
 (21) Guesdon, A.; Borel, M. M.; Grandin, A.; Leclaire, A.; Raveau, B. *J. Solid State Chem.* **1993**, *108*, 46.

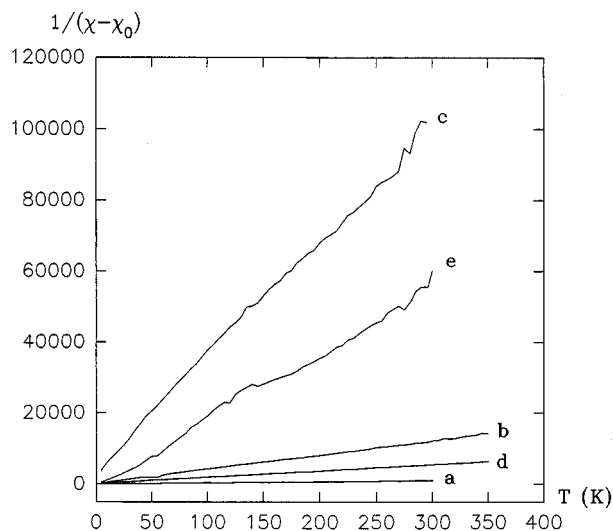


Figure 2. $1/(\chi - \chi_0)$ versus temperature for the following group 2 compounds labeled a–e: (a) $\text{Rb}_3\text{Mo}_4\text{O}_6(\text{PO}_4)_4$; (b) $\alpha\text{-K}_2\text{Mo}_2\text{O}_3(\text{PO}_4)_2$; (c) $\text{Rb}_2\text{Mo}_2\text{O}_3(\text{PO}_4)_2$; (d) $\beta\text{-K}_2\text{Mo}_2\text{O}_4(\text{P}_2\text{O}_7)$; (e) $\text{CdMoO}_2(\text{PO}_4)$. The large scattering of the moment per Mo atom deduced from the slopes of the curves is discussed in the text.

i.e., four molybdenum sites, but there are three Mo(V) and one Mo(VI) atoms distributed over the four sites. This statistic distribution of the three electrons on the four sites corresponds to the delocalization of one electron on the two octahedral sites of one of the two Mo_2O_{11} units. The resulting moment per Mo(V) atom extracted from $(\chi_M - \chi_0)^{-1}$ versus T (Figure 2) is $0.51 \mu_B$.

(b) *Class 2B₁*: For this group of the classification the biotetrahedral Mo_2O_{10} units are made from two edge-sharing octahedra (Table 2). The short Mo–Mo distance in this unit (2.62 Å) suggests the existence of a Mo–Mo chemical bond.

In $\text{CdMoO}_2(\text{PO}_4)^{32}$ as well as in $\beta\text{-K}_2\text{Mo}_2\text{O}_4(\text{P}_2\text{O}_7)^{30}$ all the molybdenum atoms have the valence Mo(V) and are engaged in Mo–Mo chemical bonds. Indeed the atomic moments per Mo atom deduced from the $(\chi_M - \chi_0)^{-1}$ versus T curves (Figure 2) are 0.17 and $0.34 \mu_B$ for the Cd- and K-based phosphates, respectively.

(c) *Class 2B₂*: Two phosphates concerned with the present work, $\text{AgMo}_3\text{O}_6(\text{PO}_4)_2$ and $\text{SrMo}_3\text{O}_6(\text{PO}_4)_2$,⁷ belong to the 2B₂ group. The same Mo_3O_{14} unit is present in the two compounds. The Mo_3O_{14} unit is built up with one Mo_2O_{10} unit (two edge-sharing octahedra) sharing one corner with a trigonal bipyramid. In the Ag-based compound there is only one Mo(V) and two

Mo(VI); on the contrary, there are two Mo(V) and one Mo(VI) in the Sr-based compound. From the $(\chi_M - \chi_0)^{-1}$ versus T curves, one finds $1.48 \mu_B$ per Mo(V) atom in the Ag compound corresponding to the behavior of one isolated Mo(V) ion. This result will be interpreted in the next section and compared to the much lower value ($0.22 \mu_B$) found for the Sr compound.

Trioctahedral Units. Four compounds concerned with the present study contain the trioctahedral unit Mo_3O_{15} . This unit is built up from a biotetrahedral unit Mo_2O_{10} which shares one oxygen of the common edge with a third octahedron. The magnetization of $\text{Cs}_9\text{Mo}_9\text{O}_3(\text{AlO}_4)_3(\text{PO}_4)_{11}$,³⁴ $\text{Rb}_9\text{Mo}_9\text{O}_3(\text{AlO}_4)_3(\text{PO}_4)_{11}$, $\text{Cs}_5\text{Rb}_4\text{Mo}_9\text{O}_3(\text{AlO}_4)_3(\text{PO}_4)_{11}$, and $\text{K}_2\text{Cs}_7\text{Mo}_9\text{O}_3(\text{AlO}_4)_3(\text{PO}_4)_{11}$ ³⁵ has been measured, and the $(\chi_M - \chi_0)^{-1}$ versus T curves fit with a magnetic moment close to $0.3 \mu_B$ per Mo(V) ion. In these compounds, all the molybdenum atoms are pentavalent. But, as will be discussed later, the molybdenum located in the two edge-sharing octahedra have their d^1 electrons engaged in a σ bond, and one can expect that the Mo_3O_{15} unit magnetically behaves as an isolated octahedron.

Tetraoctahedral Units. The tetraoctahedral unit Mo_4O_{20} is also built up from the biotetrahedral Mo_2O_{10} unit which now shares the two oxygens of the shared edge with two further octahedra. The $\text{CsMo}_2\text{O}_2(\text{PO}_4)_2$ ³⁶ phase contains Mo_4O_{20} units with mixed-valent molybdenum. The molybdenum atoms in the edge-sharing octahedra are Mo(IV), and those in the corner-sharing octahedra are Mo(V). The magnetic moment per Mo(V) atom is $0.85 \mu_B$. This value will be discussed in the next section. In $\text{Cs}_6\text{Mo}_7\text{O}_9(\text{PO}_4)_7 \cdot \text{H}_2\text{O}$ ³⁹ both the Mo_3O_{15} and Mo_4O_{20} units are present. The molybdenum valences in the Mo_4O_{20} are the same as in $\text{CsMo}_2\text{O}_2(\text{PO}_4)_2$. In the trioctahedral unit Mo_3O_{15} the three molybdenum atoms are Mo(V). The measured magnetic moment is $0.43 \mu_B$ per Mo(V) atom.

Discussion

The phases discussed in this work contain essentially two types of MoO_6 octahedra depending on the presence or not of one very strong O–Mo···O bond length alternation. As pointed out before, Mo(V) O_6 octahedra usually exhibit such a bond alternation. In this section we would like to correlate the structural and magnetic properties of the molybdenum phosphates we have investigated. The existence of MoO_6 octahedra with different valences makes necessary a detailed discussion of the real valence of each molybdenum site. We have faced this problem by using two different approaches. First, the oxidation states of the different Mo sites in the lattice have been estimated from the usual bond length–bond valence correlations.⁴⁵ Second, we have

(22) Ledain, S.; Borel, M. M.; Leclaire, A.; Provost, J.; Raveau, B. *J. Solid State Chem.* **1995**, *120*, 260.

(23) Hoareau, T.; Leclaire, A.; Borel, M. M.; Grandin, A.; Raveau, B. *J. Solid State Chem.* **1995**, *116*, 87.

(24) Costentin, G.; Borel, M. M.; Grandin, A.; Leclaire, A.; Raveau, B. *J. Solid State Chem.* **1991**, *95*, 168.

(25) Guesdon, A.; Borel, M. M.; Grandin, A.; Leclaire, A.; Raveau, B. *C. R. Acad. Sciences* **1993**, *316*, 477.

(26) Hoareau, T.; Borel, M. M.; Leclaire, A.; Provost, J.; Raveau, B. *Mater. Res. Bull.* **1995**, *30*, 523.

(27) Guesdon, A.; Leclaire, A.; Borel, M. M.; Raveau, B. *Eur. J. Solid State Inorg. Chem.* **1996**, *33*, 385.

(28) Ledain, S.; Leclaire, A.; Borel, M. M.; Raveau, B. *J. Solid State Chem.* **1996**, *122*, 107.

(29) Ledain, S.; Leclaire, A.; Borel, M. M.; Raveau, B. *J. Solid State Chem.*, in press.

(30) Guesdon, A.; Leclaire, A.; Borel, M. M.; Grandin, A.; Raveau, B. *J. Solid State Chem.* **1995**, *114*, 481.

(31) Mundi, L. A.; Haushalter, R. *Inorg. Chem.* **1990**, *29*, 2879.

(32) Guesdon, A.; Leclaire, A.; Borel, M. M.; Raveau, B. *J. Solid State Chem.* **1996**, *122*, 343.

(33) Hoareau, T.; Leclaire, A.; Borel, M. M.; Raveau, B., to be published.

(34) Guesdon, A.; Borel, M. M.; Leclaire, A.; Grandin, A.; Raveau, B. *J. Solid State Chem.* **1995**, *114*, 451.

(35) Guesdon, A.; Leclaire, A.; Borel, M. M.; Raveau, B. *Chem. Mater.* **1995**, *7*, 1873.

(36) Guesdon, A.; Borel, M. M.; Leclaire, A.; Grandin, A.; Raveau, B. *Z. Anorg. Allg. Chem.* **1993**, *619*, 1841.

(37) King, H. E.; Mundi, L. A.; Strohmaier, K. G.; Haushalter, R. C.; *J. Solid State Chem.* **1991**, *92*, 1.

(38) Leclaire, A.; Borel, M. M.; Grandin, A.; Raveau, B. *J. Solid State Chem.* **1993**, *108*, 46.

(39) Guesdon, A.; Borel, M. M.; Leclaire, A.; Grandin, A.; Raveau, B. *J. Solid State Chem.* **1994**, *111*, 315.

carried out tight-binding calculations for the 3D lattices and/or molecular orbital calculations for fragments of them in order to discuss in detail the nature of the electronic levels.⁴⁶ As noted in the section concerning the magnetic measurements, the effective magnetic moments per Mo(V) in several of these phases are noticeably smaller than expected. Even if some type of nonstoichiometry could be invoked to explain these observations, the differences are sometimes too large to always give credit to such an explanation. In some cases the unpaired electrons associated with some Mo^{VO}_6 octahedra must be strongly coupled leading to an effective decrease of the magnetic moment. For instance, this possibility is quite clear in the case of phases containing biotetrahedral units built from edge-sharing octahedra.

The t_{2g} levels of a regular MoO_6 octahedron have antibonding combinations between the Mo d orbitals and the O p orbitals. Hence, a shortening of an Mo–O bond length raises the energy of any t_{2g} orbital if it has an antibonding combination between the Mo and O orbitals along the shortened Mo–O bond. Consequently, a distortion where one Mo–O bond is shortened leaves one t_{2g} level (i.e., that which is in a plane perpendicular to the shortened Mo–O bond) and raises the energy of the remaining two levels (see Figure 3a). By contrast, all three t_{2g} levels are raised by a distortion in which two or more Mo–O bonds are shortened.⁴⁷ In fact, the situation depicted in Figure 3a applies to all Mo(V) octahedra we consider here. Then, just by carefully considering the crystal structure and using this qualitative reasoning, we can determine the directionality of the orbitals associated with the d electrons of the $\text{Mo(V)}\text{O}_6$ octahedra and we can analyze if there is some possibility of coupling.

The values of μ_B found for the two phases containing isolated octahedral units which we have studied are somewhat different: 1.73 for KMoOP_2O_7 and 1.30 for $\text{CsMoOP}_2\text{O}_7$. Whereas the first value is what is expected for an isolated Mo^{VO}_6 , the second seems to be too small. Our calculations for the 3D networks of the two related but slightly different structures exclude any coupling between the low-lying t_{2g} orbital of the different octahedra either directly or through the PO_4 tetrahedra. We believe the more plausible origin for the relatively low value of μ_B for $\text{CsMoOP}_2\text{O}_7$ should lie in

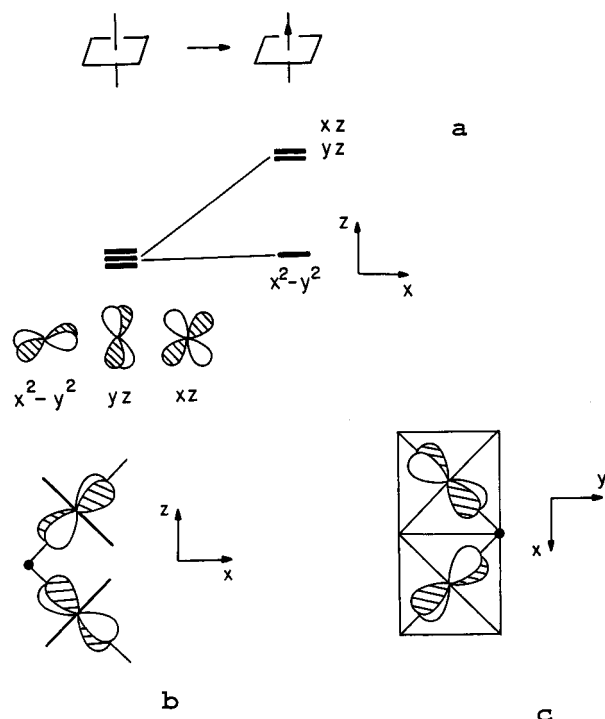


Figure 3. (a) Schematic representation of the energy level of the t_{2g} orbitals of a regular MoO_6 octahedron (left) and of a MoO_6 exhibiting a strong apical bond alternation (right). The arrow shows the shorter $\text{Mo}\cdots\text{O}$ apical distance. (b) Lowest lying orbital in the Mo_2O_{11} unit (two octahedra sharing one corner). The dot indicates the absence of oxygen contribution in one site. (c) Lowest lying orbital in the Mo_2O_{10} unit (two octahedra sharing one edge).

some difference in the stoichiometry between the two oxides even if such a difference has not been evidenced on the small-sized single crystals used in the X-ray diffraction study.

Compounds belonging to class 2A exhibit Mo_2O_{11} units made of two corner-sharing octahedra. The calculated valences⁴⁵ for the two Mo atoms of these units are 5.01/5.02 for $\alpha\text{-K}_2\text{Mo}_2\text{O}_3(\text{PO}_4)_2$ and 4.84/4.99 for $\alpha\text{-Rb}_2\text{Mo}_2\text{O}_3(\text{PO}_4)_2$. Thus the two sites have the same valence (V). For $\text{Rb}_3\text{Mo}_4\text{O}_6(\text{PO}_4)_4$ there are two different Mo_2O_{11} units but only three electrons. The calculated valences⁴⁵ for the two Mo atoms of each unit are 5.4/5.5 and 5.3/5.3. These results suggest a statistical distribution of biotetrahedral units with $\text{Mo(V)}/\text{Mo(V)}$ and $\text{Mo(V)}/\text{Mo(VI)}$.

The strong O–Mo \cdots O alternation in these three compounds occurs with two of the four equatorial oxygen atoms. Thus, the low-lying t_{2g} orbital is one that can make π -type interactions with the p_y orbital of the shared oxygen atom. However, as shown in Figure 3b, the out-of-phase combination of the two t_{2g} orbitals cannot mix with the p_y orbital of the bridging oxygen because of the local pseudosymmetry plane and lies at low energy (for simplicity we do not show the orbitals of the nonshared oxygens and we use a dot to indicate the absence of oxygen contribution in one site). The in-phase combination of the two t_{2g} orbitals can mix with the p_y orbital of the bridging oxygen and thus lies at higher energies. According to our calculations the energy gap between the two orbitals is always around 0.5 eV. Consequently, the two electrons per Mo_2O_{11} unit of $\alpha\text{-K}_2\text{Mo}_2\text{O}_3(\text{PO}_4)_2$ and $\alpha\text{-Rb}_2\text{Mo}_2\text{O}_3(\text{PO}_4)_2$ are housed in the low-lying orbital (Figure 3b), and thus a diamag-

(40) Hoareau, T.; Leclaire, A.; Borel, M. M.; Grandin, A.; Raveau, B. *Eur. J. Solid State Inorg. Chem.* **1994**, *31*, 727.

(41) Borel, M. M.; Chardon, J.; Leclaire, A.; Grandin, A.; Raveau, B. *J. Solid State Chem.* **1994**, *112*, 317.

(42) Lii, K. H.; Johnston, D. C.; Goshorn, D. P.; Haushalter, R. C. *J. Solid State Chem.* **1987**, *71*, 131.

(43) Kierkegaard, P.; Longo, J. M. *Acta Chem. Scand.* **1970**, *24*, 427.

(44) Leclaire, A.; Borel, M. M.; Grandin, A.; Raveau, B. *Z. Kristallog.* **1990**, *190*, 135.

(45) Brown, I. D.; Altermatt, D. *Acta Crystallogr.* **1985**, *B41*, 244.

(46) Both the tight-binding and molecular calculations are of the extended Hückel type (Hoffmann, R. *J. Chem. Phys.* **1963**, *39*, 1397). The off-diagonal matrix elements of the Hamiltonian were calculated according to the modified Wolfsberg–Helmholz formula (Ammeter, J.; Bürgi, H.-B.; Thibault, J.; Hoffmann, R. *J. Am. Chem. Soc.* **1978**, *100*, 3686). The exponents and parameters used in our calculations are as follows: 2.275 and –32.3 eV for O 2s, 2.275 and –14.8 eV for O 2p, 1.75 and –19.0 eV for P 3s, 1.75 and –12.0 eV for P 3p, 1.20 and –4.34 eV for K 4s, 1.20 and –2.73 eV for K 4p, 1.26 and –3.88 eV for Cs 6s, 1.26 and –2.49 eV for Cs 6p, 1.96 and –8.34 eV for Mo 5s, 1.90 and –5.24 eV for Mo 5p. The 4d orbitals of Mo were represented as a linear combination of two Slater orbitals. The associated valence-state ionization potential, exponents, and coefficients used were –10.50, 4.54, 1.90, 0.5899, and 0.5899, respectively.

(47) Canadell, E.; Whangbo, M.-H. *Chem. Rev.* **1991**, *91*, 965.

netic behavior is expected. For $\text{Rb}_3\text{Mo}_4\text{O}_6(\text{PO}_4)_4$ there are three electrons per two different Mo_2O_{11} units. Our calculations for the two types of Mo_2O_{11} units give practically identical results. In both cases the low-lying orbital (Figure 3b) is energetically well separated from the next orbital and is equally shared by the two molybdenum atoms. Consequently, there must be a statistical distribution of bioctahedral units with one pair of strongly coupled electrons and of bioctahedral units with one unpaired electron delocalized among the two sites. Thus, in agreement with the results of the previous section, the effective magnetic moment per Mo(V) atom is expected to be one-third of the theoretical value.

The $\text{CdMoO}_2(\text{PO}_4)$, $\beta\text{-K}_2\text{Mo}_2\text{O}_4(\text{P}_2\text{O}_7)$, $\text{AgMo}_3\text{O}_6(\text{PO}_4)_2$, and $\text{SrMo}_3\text{O}_6(\text{PO}_4)_2$ phases they all have edge-sharing Mo_2O_{10} bioctahedral units, although the latter two share one of the oxygen atoms with a MoO_5 pentagonal bipyramid (class $2B_2$). Both the molecular orbital calculations and the bond length–bond valence correlations suggest that the Mo in the pentagonal bipyramid is in a +VI oxidation state. The presence of the pentagonal bipyramid in the class $2B_2$ phases induces a subtle change in the internal geometry of the octahedra. Whereas those of the $\text{CdMoO}_2(\text{PO}_4)$ and $\beta\text{-K}_2\text{Mo}_2\text{O}_4(\text{P}_2\text{O}_7)$ phases (class $2B_1$) have a strong alternation perpendicular to the equatorial plane, those of class $2B_2$ phases have the strong alternation within the plane of the equatorial oxygens. In the first case, the low-lying t_{2g} orbital is the $x^2 - y^2$ (see Figure 3a), which is well oriented to interact in a σ way with the $x^2 - y^2$ orbital of the second octahedra. This leads to a low-lying orbital which according to our calculations is in both cases well separated from the next energy level (~ 0.85 eV). Thus the two electrons of the biocahedral units of these class $2B_1$ phases are strongly coupled, leading to a Mo–Mo σ bond. Consequently these phases should be nearly diamagnetic.

The number of Mo(V) sites in the two class $2B_2$ phases investigated here is different: there are two for $\text{SrMo}_3\text{O}_6(\text{PO}_4)_2$ but only one for $\text{AgMo}_3\text{O}_6(\text{PO}_4)_2$. In the second case, the bond length–bond valence calculations⁴⁵ give 5.83 for the valence of the Mo site which shares an oxygen with the pentagonal bipyramid (Mo(2)) and 5.12 for the other (Mo(1)). This suggests that the electron of the biocahedral unit is localized in the Mo(1) site. Interestingly, with two Mo(V) sites and a long Mo–Mo distance (3.37 Å), $\text{SrMo}_3\text{O}_6(\text{PO}_4)_2$ is not expected to be nearly diamagnetic as found in our magnetic measurements.

As mentioned, the O–Mo···O bond alternation of these class $2B_2$ phases occurs not in a direction perpendicular to the equatorial plane of the octahedra but within such plane. The low-lying t_{2g} orbital lies in a plane perpendicular to the equatorial one and points toward one of the shared positions of the biocahedral unit. Thus, this orbital is different from that of the biocahedral units of the $\text{CdMoO}_2(\text{PO}_4)$ and $\beta\text{-K}_2\text{Mo}_2\text{O}_4(\text{P}_2\text{O}_7)$ phases. The local symmetry of the out-of-phase combination of the two orbitals (Figure 3c) does not allow the mixing of the p_z orbital of the shared oxygen toward which they point, and consequently this orbital lies at low energy. The in-phase combination of the two orbitals allows the mixing of the p_z orbital of the shared oxygen and lies at higher energies. According to our computations the orbital of the Figure 3c is the lowest

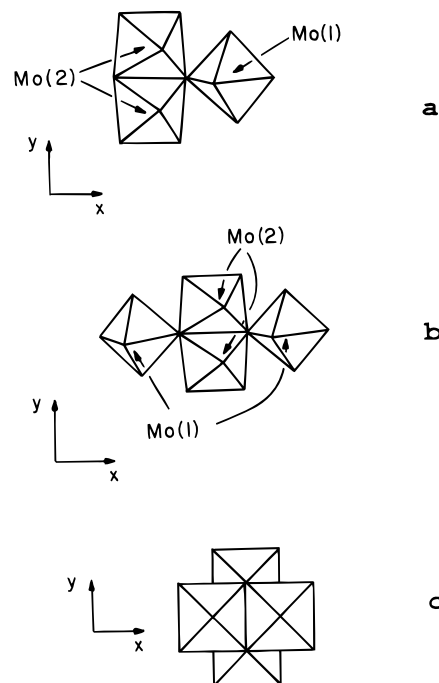


Figure 4. (a) Trioctahedral unit Mo_3O_{15} with the Mo(2) and Mo(1) sites (see text). (b) The tetraoctahedral unit Mo_4O_{20} in which the Mo(2)O_6 octahedra are very regular and the Mo(1)O_6 octahedra show a strong O–Mo···O bond alternation. (c) Tetraoctahedral unit Mo_4O_{16} built on two Mo_2O_{10} units sharing four edges. In this Mo_4O_{16} unit all the octahedra show a O–Mo···O bond alternation perpendicular to the equatorial plane of the two Mo_2O_{10} units.

lying of the biocahedral unit and is well separated (~ 0.4 – 0.5 eV) from both the next level of the biocahedra and the lower level of the pentagonal bipyramid. The only difference in our calculations for the $\text{SrMo}_3\text{O}_6(\text{PO}_4)_2$ and $\text{AgMo}_3\text{O}_6(\text{PO}_4)_2$ is that whereas in the first case the orbital (Figure 3c) is almost equally distributed among the two molybdenum sites of the Mo_2O_{10} unit, in $\text{AgMo}_3\text{O}_6(\text{PO}_4)_2$ it is heavily concentrated on the Mo(1) atom (i.e., 71% of the orbital is concentrated on Mo(1) and only 21% on the Mo(2)) because of the stronger distortion of the Mo(2)O_6 octahedra. Consequently, the two electrons of the biocahedral units of $\text{SrMo}_3\text{O}_6(\text{PO}_4)_2$ are strongly coupled, and the phase should be nearly diamagnetic. It is interesting to emphasize that this is so despite the very long Mo–Mo distance (3.37 Å) which rules out the existence of a Mo–Mo bond. As for the Mo_2O_{11} biocahedral units of the $\text{K}_2\text{Mo}_2\text{O}_3(\text{PO}_4)_2$ and $\alpha\text{-Rb}_2\text{Mo}_2\text{O}_3(\text{PO}_4)_2$ phases, the coupling is not a direct coupling but through the p orbital of one bridging oxygen. For $\text{AgMo}_3\text{O}_6(\text{PO}_4)_2$ our calculations confirm that the valences are localized and the unpaired electron resides on the Mo(1)O_6 octahedra.

The trioctahedral units of the $\text{Ag}_9\text{Mo}_9\text{O}_3(\text{AlO}_4)_3(\text{PO}_4)_{11}$ phases we have studied are built from an edge-sharing Mo_2O_{10} unit which shares one of its common oxygens with another octahedron (Figure 4a). We will refer to the two equivalent Mo atoms of the biocahedral unit as Mo(2) and to that of the third octahedron as Mo(1). Using the structure of $\text{Cs}_9\text{Mo}_9\text{O}_3(\text{AlO}_4)_3(\text{PO}_4)_{11}$, the calculated valences⁴⁵ for Mo(1) and Mo(2) are 4.99 and 4.85, respectively. Thus all octahedra can be described as Mo(V)O_6 . The strong alternation for the two octahedra of the Mo_2O_{10} unit occurs along the direction perpendicular to the equatorial plane. Thus the situ-

ation is exactly as for the phases of class 2B₁ examined above: the low-lying t_{2g} orbital is $x^2 - y^2$, which points toward the $x^2 - y^2$ orbital of the second Mo atom of the bioctahedral unit and leads to a Mo–Mo σ bonding orbital. This orbital is well separated (0.7 eV) from the next orbital of the trioctahedral unit which is the lowest t_{2g} orbital of the Mo(1)O₆ octahedron. Consequently, the two electrons of the Mo(V)O₆ octahedra of the edge-sharing bioctahedral unit are strongly coupled, and there is only one unpaired electron per trioctahedral unit located on the Mo(1)O₆ octahedron. The value of the effective magnetic moment per Mo(V) atom is thus expected to be one-third of the theoretical value. Although the observed values are somewhat smaller, our calculations do not support the possibility of coupling between the low-lying Mo(1)O₆ t_{2g} orbitals of different trioctahedral units, either directly or through the PO₄ tetrahedra.

Let us now consider the tetraoctahedral units built from the edge-sharing Mo₂O₁₀ bioctahedral unit, which shares two of the common oxygens with two further octahedra (Figure 4b). Phases containing such units include CsMo₂O₂(PO₄)₂, K_{1.5}Mo₂O₂(PO₄)₂·H₂O, and Cs₆-Mo₇O₉(PO₄)₇·H₂O. The Mo(2)O₆ octahedra are very regular whereas the Mo(1)O₆ ones have a strong O–Mo···O bond alternation within the equatorial plane (here we consider the triply shared oxygen as an apical vertex of the Mo(1)O₆ octahedra but an equatorial vertex of the Mo(2)O₆ ones). Using the crystal structure of CsMo₂O₂(PO₄)₂, the calculated valences⁴⁵ for the Mo(1) and Mo(2) atoms are 4.96 and 3.96, respectively. This suggests the oxidation states V and IV for Mo(1) and Mo(2), respectively. Since there is no O–Mo···O bond alternation in the Mo(2)O₆ octahedra the three t_{2g} orbitals are low in energy and lead to a set of three bonding (σ , π , and δ) and three antibonding (σ^* , π^* , and δ^*) orbitals for the edge-sharing bioctahedral unit. Our calculations for the tetraoctahedral units of CsMo₂O₂(PO₄)₂ show that there are two low-lying orbitals (mainly the σ and π of the edge-sharing bioctahedral unit) separated by a gap of 0.5 eV from the next two levels which are essentially the low-lying t_{2g} orbitals of each of the two Mo(1)O₆ octahedra. Thus, these calculations show that there is a Mo(2)=Mo(2) double bond and confirm the oxidation states proposed above. In K_{1.5}Mo₂O₂(PO₄)₂·H₂O there is one more electron per tetraoctahedral unit. Our calculations show that in that case the δ orbital of the edge-sharing bioctahedral unit is slightly below the low-lying t_{2g} levels of each of the two Mo(1)O₆ octahedra. Thus the extra electron is delocalized between the two Mo(2)O₆ octahedra leading to a half integer oxidation state (+3.5). The situation here is completely different from AgMo₃O₆(PO₄)₂ where the two octahedra of the edge-shared Mo₂O₁₀ unit exhibit different oxidation states (V and VI).

Our calculations for the tetraoctahedral units of CsMo₂O₂(PO₄)₂ suggest that there is one unpaired electron per Mo(V)O₆ octahedra. The measured magnetic moment per Mo(V) atom is around half the expected value. This difference is obviously too large to be due to nonstoichiometry problems. Our calculations for the tetraoctahedral units of CsMo₂O₂(PO₄)₂, K_{1.5}Mo₂O₂(PO₄)₂·H₂O, and Cs₆Mo₇O₉(PO₄)₇·H₂O show that the low-lying t_{2g} levels of the two Mo(1)O₆ octahe-

dra lie energetically very near the δ and δ^* orbitals of the edge-shared bioctahedral unit. These orbitals can provide a coupling path between the low-lying t_{2g} levels of the two Mo(V)O₆ octahedra. Although this coupling is weak according to our calculations, it can be very sensitive to the energy separation between the δ/δ^* and the low t_{2g} levels of the two Mo(V)O₆ octahedra. We believe that weak coupling through the δ/δ^* levels of the bioctahedral unit can be the reason for the decreased values of the magnetic moment per Mo(V) in the phases containing tetraoctahedral units such as that shown in Figure 4b.

Although we have not studied the magnetic properties of BaMo₄O₈(PO₄)₂ (class 4B) involving only Mo(V), we have carried out calculations for the Mo₄O₁₆ units (Figure 4c) of this phase. In Figure 4c two Mo₂O₁₀ bioctahedral units share four edges, and all octahedra have an O–Mo···O bond alternation perpendicular to the equatorial plane of the Mo₂O₁₀ units. Thus the t_{2g} orbital which lies at low energy is $x^2 - y^2$. This orbital is well oriented to interact with the other $x^2 - y^2$ orbital of the same Mo₂O₁₀ unit leading to a Mo–Mo σ bond. At the same time it almost does not interact with those of the other Mo₂O₁₀ unit. Thus we should expect the existence of two low-lying orbitals associated with a Mo–Mo σ bond of each of the two Mo₂O₁₀ units. In agreement with this qualitative analysis, our calculations for the Mo₄O₁₆ units of BaMo₄O₈(PO₄)₂⁴¹ show that there are two low-lying Mo–Mo bonding orbitals separated by a large energy gap (1 eV) from the next orbitals. Thus it is predicted that BaMo₄O₈(PO₄)₂ will be diamagnetic.

Finally let us consider MoAlP₂O₉, which contains infinite chains of corner-sharing Mo(V)O₆ octahedra. It is interesting to compare this phase with α -Rb₂Mo₂O₃-(PO₄)₂ which contains corner-sharing bioctahedral units. With an infinite chain of Mo(V)O₆ octahedra there is in principle the possibility of electronic delocalization along the chain and thus metallic character. It all depends on the nature of the O–Mo···O bond alternation. In MoAlP₂O₉ the alternation occurs along the chain direction. Thus the low-lying t_{2g} orbital is $x^2 - y^2$, which makes δ -type interactions along the chain, and thus it cannot interact with any of the oxygen orbitals. Consequently, the unpaired electron of each Mo(V)O₆ octahedron is completely localized, and this phase should be paramagnetic. The difference with α -Rb₂Mo₂O₃-(PO₄)₂ arises from the fact that in the latter the strong O–Mo···O bond alternation implicates two equatorial oxygen atoms instead of two apical ones. This changes the nature of the low-lying t_{2g} orbital which in α -Rb₂-Mo₂O₃(PO₄)₂ makes π -type interactions with the oxygen p orbitals leading to delocalization. This example makes clear that although the PO₄ tetrahedra do not effectively couple the unpaired electrons of the different Mo^{VO} octahedra, they can play an important role in determining the magnetic properties of these phases by influencing the direction of the O–Mo···O bond alternation within the octahedra.

Concluding Remarks

The number of molybdenum phosphates containing Mo(V) either as purely Mo(V) or as mixed valent Mo(IV/V) and Mo(V/VI) has greatly increased in recent years. The frameworks of these phases contain octa-

hedral units built from several octahedra through corner or edge sharing. The more convenient structural classification of these phases seems to be according to the number of octahedra in these units. A combined theoretical and magnetic study of several of these phases led us to the elucidation of the valence of the different Mo atoms in these systems as well as to show the different possibilities of coupling for the unpaired electron of the Mo(V) octahedra. The PO₄ tetrahedra, which do not effectively couple the unpaired electrons of the

different Mo(V)O₆ octahedra, play an important role in determining the magnetic properties of these solids by influencing the internal geometry of the MoO₆ octahedra.

Acknowledgment. E.C. would like to thank the CNRS for a sabbatical which made the stay at the ICMAB possible.

CM960161V